THE JOURNAL OF BIOLOGICAL CHEMISTRY VOL. 283, NO. 25, pp. 17605–17614, June 20, 2008

Regulation of TIP60 by ATF2 Modulates ATM Activation*[S]

Received for publication, March 13, 2008, and in revised form, April 4, 2008 Published, JBC Papers in Press, April 8, 2008, DOI 10.1074/jbc.M802030200

Anindita Bhoumik[‡], Netai Singha[‡], Matthew J. O'Connell[§], and Ze'ev A. Ronai[‡1]

From the [‡]Signal Transduction Program, Burnham Institute for Medical Research, La Jolla, California 92037 and the [§]Department of Oncological Sciences, Mount Sinai School of Medicine, New York, New York 10029

TIP60 (HTATIP) is a histone acetyltransferase (HAT) whose function is critical in regulating ataxia-telangiectasia mutated (ATM) activation, gene expression, and chromatin acetylation in DNA repair. Here we show that under non-stressed conditions, activating transcription factor-2 (ATF2) in cooperation with Cul3 ubiquitin ligase promotes degradation of TIP60, thereby attenuating its HAT activity. Inhibiting either ATF2 or Cul3 expression by small interfering RNA stabilizes the TIP60 protein. ATF2 association with TIP60 on chromatin is decreased following exposure to ionizing radiation (IR), resulting in enhanced TIP60 stability and activity. We also identified a panel of melanoma and prostate cancer cell lines whose ATF2 expression is inversely correlated with TIP60 levels and ATM activation after IR. Inhibition of ATF2 expression in these lines restored TIP60 protein levels and both basal and IR-induced levels of ATM activity. Our study provides novel insight into regulation of ATM activation by ATF2-dependent control of TIP60 stability and activity.

The nuclear protein kinase ataxia-telangiectasia mutated (ATM)[2] belongs to the phosphatidylinositol 3-kinase-like kinase family (1), which is activated in response to genotoxic insults that elicit double-stranded DNA breaks (DSBs) (2). Consequently, ATM phosphorylates several proteins implicated in control of genome integrity (3, 4). Among them are the checkpoint signaling kinases Chk2 and Chk1 (5, 6), checkpoint mediators ATF2, BRCA1, 53BP1, and MDC1 (7–10), the histone variant H2AX, and diverse effectors of the DNA damage network involved in DNA repair, cell cycle, and cell death control including RAD9, RAD17, SMC1, FANCD2, and p53 (11–14).

DNA damage activates signal transduction pathways that rapidly affect processes such as transcription, cell cycle progression, and DNA replication (15). Common to these processes are alterations in chromatin structure. Post-translational modifications of histones including acetylation, ubiquitination, and phosphorylation have emerged as key regulatory events controlling the DNA damage response. For example, the N terminus of histones H3 and H4 is subject to reversible acetylation that affects expression of enzymes involved in DNA repair and sensitivity to DNA-damaging agents (16–19).

Initially discovered as a Tat-interacting protein, TIP60 is a chromatin-modifying enzyme and key component of repair and antiproliferative responses to DNA damage (17, 20). TIP60 elicits such control via acetylation of histones in the vicinity of lesions during DNA repair (17). The *Drosophila* homolog dTIP60 acetylates nucleosomal phospho-H2Av, promoting its exchange with unmodified H2Av (21). The yeast homolog Esa1 (essential SAS2-related acetyltransferase) acetylates histone H4 (22). These events are required for DNA repair in both flies and yeast. TIP60 accumulates in cells exposed to ultraviolet (UV) irradiation (23) and is required for DNA repair and apoptosis following IR (17). Suppression of TIP60 abolishes G_1 cell cycle arrest induced by IR (20). Interestingly, TIP60 activates ATM following genotoxic stresses, linking detection of DNA breaks to checkpoint and DNA repair responses (24).

The HAT cofactor TRRAP and TIP60 bind to chromatin-surrounding sites of DSBs *in vivo* (25). The Trrap/TIP60 complex also includes TIP49a and TIP49b (17), members of a family of AAA^+ ATPases functioning in DNA repair, recombination, and transcriptional regulation (26). We previously identified TIP49b as an ATF2-associated protein that limits ATF2 transcriptional activities in response to UV or IR (27). ATF2 was also shown to be phosphorylated by ATM, enabling it to mediate the intra-S phase checkpoint as well as co-localize with the MRE11 complex within DSB foci following IR (8). Intriguingly, inhibiting ATF2 expression attenuates ATM activation following IR, suggesting a reciprocal relationship between the two proteins (8). Here we disclose the mechanism underlying the effect of ATF2 on ATM activity.

EXPERIMENTAL PROCEDURES

Cells—HeLa and HEK293T cells were maintained in Dulbecco's modified Eagle's medium supplemented with calf serum (10%) and antibiotics. WM115, WM793, FEMX, HHMSX, WIDR, A549, PC3, LNcaP, ALav31, and M12 cells were grown in RPMI 1640 media supplemented with 10% fetal bovine serum and antibiotics.

Plasmids and Transfection—Plasmids expressing both wild type and mutant forms of HA-ATF2 were described previously (8). PCR-amplified TIP60 cDNA (17) was subcloned into the BamHI and NotI sites of the PEF-FLAG vector. TIP60 deletion mutants were generated by PCR and subcloned into PEF-FLAG vector. Plasmid integrity was confirmed by sequencing. pcDNA3 Myc-tagged Cullin3 and pcDNA3 HA-ROC1 were

* This work was supported, in whole or in part, by National Institutes of Health Grants CA 099961 (to Z. R.) and CA100076 (to M. O. C.). The costs of publication of this article were defrayed in part by the payment of page charges. This article must therefore be hereby marked "*advertisement*" in accordance with 18 U.S.C. Section 1734 solely to indicate this fact.

[S] The on-line version of this article (available at http://www.jbc.org) contains supplemental Figs. S1–S4.

[1] To whom correspondence should be addressed. Tel.: 858-646-3185; E-mail: ronai@burnham.org.

[2] The abbreviations used are: ATM, ataxia-telangiectasia mutated; DSB, double-stranded DNA break; HA, hemagglutinin; HAT, histone acetyltransferase; RNAi, RNA interference; RT, reverse transcriptase; siRNA, small interfering RNA; JNK, c-Jun N-terminal kinase.

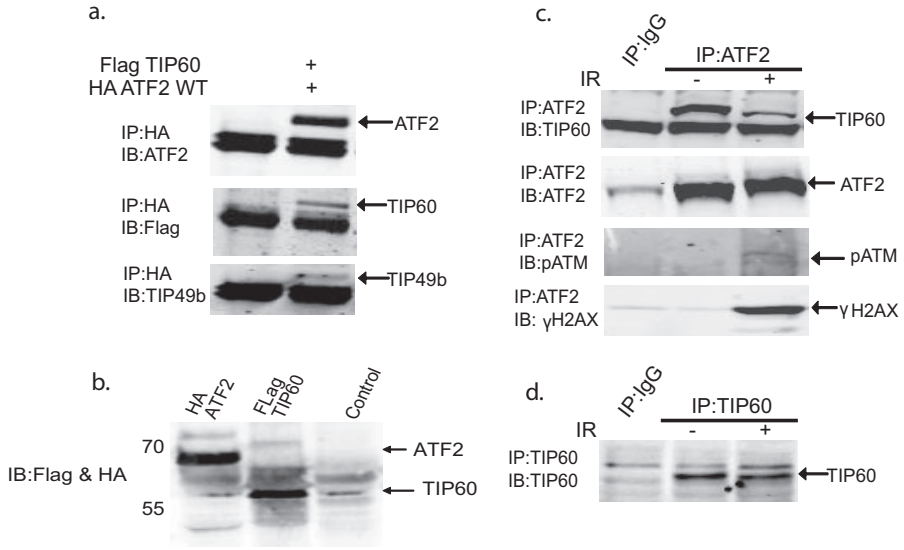

FIGURE 1. **ATF2 interacts with the TIP60 complex.** *a*, FLAG-TIP60 is immunoprecipitated with HA-ATF2. 293T cells were transfected with FLAG-tagged TIP60 and HA-tagged ATF2. 24 h after transfection cells were harvested and the nuclear fraction subjected to immunoprecipitation (*IP*) followed by immunoblotting (*IB*) with the indicated antibodies to assay for ATF2 association with TIP60 or endogenous TIP49b. *b*, input levels of ATF2 and TIP60 used in *panel a*. *c*, ATF2 association with endogenous TIP60 is reduced following IR. WIDR cells were mock treated or irradiated (10 Gray). 1 h post-irradiation cells were harvested and chromatin-enriched fractions prepared. IP followed by IB was carried out with the indicated antibodies. *d*, endogenous levels of TIP60 in extracts used in *panel c*.

kindly provided by Z. Q. Pan. Plasmids were transfected into 293T cells using the calcium phosphate method and into HeLa, WM793, and M12 cells using Lipofectamine Plus (Invitrogen).

Reagents and Antibodies—Antibodies were purchased as follows: anti-TIP60, anti-phospho-SMC1, anti-SMC1, anti-H2AX, anti-γH2AX, anti-Ac H4 K16 antibodies, anti-Ac H4 K5 from Upstate Biotechnology; anti-ATF2 from Santa Cruz; anti-Ser(P)1981 ATM from Rockland Immunochemicals; anti-TIP49b from BD Biosciences; anti-HA Ab 12CA5 from Covance; and anti-FLAG and anti-β-Actin antibodies from Sigma. A mouse monoclonal antibody against ATM (MAT3) was a kind gift from Y. Shiloh. For immunoprecipitation, TIP60 polyclonal antibody was generated using full-length, bacterially produced TIP60 (EMD Biosciences, San Diego, CA). MG132 was purchased from Boston Biochemicals and sodium butyrate was purchased from Sigma.

RNA Interference—For RNAi targeting of *ATF2* and *TIP60*, the pSuper vector system that directs synthesis of siRNAs in mammalian cells was used (28). The target was ^{523}GTTGGCGAGTCCATTTGAG^{541} of the human *ATF2* gene (accession number NM_001880). The TIP60 target sequence for RNAi was ^{543}ACGGAAGGTGGAGGTGGTT^{561} of human *TIP60* (accession number NM_182710). Oligonucleotides were annealed and ligated into BglII and HindIII sites of pSuper vector to construct pS-ATF2 and pS-TIP60. To target *CULLIN3*, corresponding SMARTpool siRNA reagents were used. As a control, the corresponding siRNA control oligo was used (Dharmacon). Transfection of siRNA duplexes was carried out using oligofectamine and the pSuper vector with Lipofectamine Plus (Invitrogen). ATF2 and TIP60 expression levels were measured 48 h after transfection.

RT-PCR Analyses—Cells treated with or without IR were harvested and total RNA extracted using an RNA extraction kit (Sigma). Complementary DNA was synthesized from 2.5 μg of total RNA using an oligo(dT) (19) primer. Primers used for PCR were TIP60 forward: 5′-ATGAGCGGCTGGACCTAAAGAAGA-3′ and reverse 5′-AGTCCTCATCAGTGCCCAAACAAT-3′; and glyceraldehyde-3-phosphate dehydrogenase forward 5′-ACCACAGTCCATGCCATCAC-3′ and reverse 5′-TCCACCACCCTGTTGCTGTA-3′. Amplification of TIP60 and glyceraldehyde-3-phosphate dehydrogenase required 20 and 18 cycles, respectively. Products were analyzed on 1.5% agarose gels.

Chromatin-bound Fractionation and Immunoblotting—Irradiated or mock-treated cells were washed twice with ice-cold phosphate-buffered saline, and cell fractionation was carried out by three consecutive extractions. In brief, 3×10^8 cells were first resuspended 5 min on ice in 500 μl of fractionation buffer (50 mM Tris, pH 7.5, 50 mM NaCl, and 0.5% Nonidet P-40 supplemented with protease and phosphatase inhibitors) to isolate the cytoplasmic fraction. After centrifugation, the supernatant was collected (fraction I), and pellets containing nuclei were washed twice with the same buffer. Nuclei were further extracted for 40 min on ice with 350 μl of fractionation buffer containing 50 mM Tris, pH 7.5, 150 mM NaCl, and 0.5% Nonidet P-40 supplemented with protease and phosphatase inhibitors. After rotating at 4 °C for 30 min, samples were centrifuged at 13,200 × *g* for 30 min. The supernatant was saved as the nuclear extract (fraction II). The nuclear pellet was lysed using fractionation buffer containing 50 mM Tris, pH 7.5, 150 mM NaCl, 0.5% Nonidet P-40 supplemented with protease and phosphatase inhibitors and DNase I (0.1 mg/ml) followed by sonication. The supernatant was treated with 0.1 mg/ml EtBr for 10 min and extracts centrifuged at 14,000 × *g* for 20 min at 4 °C. Supernatants were collected as the chromatin-enriched fraction (fraction III).

HAT Activity Assay—FLAG-tagged TIP60 bound to chromatin was isolated as described above. Radioactive HAT filter binding assays were performed as described (29) with minor modifications. Samples were incubated at 30 °C for 60 min in 30 μl of assay buffer containing 50 mM Tris-HCl, pH 8.0, 10% glycerol, 1 mM dithiothreitol, 1 mM phenylmethylsulfonyl fluoride, 10 mM sodium butyrate, 90 pmol of [^{3}H]acetyl-CoA (3.3 Ci mmol^{-1}; PerkinElmer Life Sciences), 2 pmol of TIP60 complex, and 1 μg of bacterially produced recombinant human histone H4 (Upstate Biotechnologies). After incubation, the reaction mixture was spotted onto Whatman P-81 phosphocellulose filter paper and washed for 30 min with 0.2 M sodium carbonate buffer, pH 9.2, at room temperature with 2–3 buffer changes. Dried filters were counted in a liquid scintillation counter. For a non-radioactive HAT assay, immunoprecipitates were incu-

bated in 60 μl of HAT assay buffer containing acetyl-CoA (100 μM), 1 pmol of TIP60 complex, and biotinylated histone H4 peptide (0.5 μg) for 30 min at 30 °C. An aliquot of the reaction was immobilized onto streptavidin plates and acetylation was detected by a HAT ELISA according to the manufacturer's instructions (Upstate Biotechnology).

Immunoblotting and Quantitation—Proteins were separated on 4–20% gradient gels and blotted onto nitrocellulose membranes. Alexa Fluor 680 anti-rabbit and anti-mouse and IRdye800 anti-mouse secondary antibodies were obtained from Invitrogen and Rockland Immunochemicals, respectively. The use of infrared fluorescent dyes on the secondary antibodies allows direct quantitation of secondary antibodies using the Odyssey system (Licor). Membranes were scanned and quantified using this system and associated software.

Immunostaining—Cells were plated on coverslips and irradiated, fixed at the indicated time points, and processed as described (8).

Pulse-Chase—Cells were washed and incubated with methionine/cysteine-free media (45 min at 37 °C). Medium was then replaced with methionine/cysteine-free medium supplemented with 100 μCi of [^{35}S]methionine/cysteine per ml. After 45 min incubation with radioactive medium (pulse), cells were washed and incubated with methionine/cysteine-containing medium for the indicated time points (chase). Cell extracts were subject to IP as detailed above.

RESULTS

ATF2 Associates with TIP60—Ectopically expressed ATF2 and TIP60 were shown to associate following immunoprecipitation of ATF2 (Fig. 1, *a* and *b*). Other components of this complex included endogenous TIP49b. Importantly, analysis of the chromatin-bound fraction revealed association of endogenous TIP60 with endogenous ATF2 prior to IR (Fig. 1*c*). The amount of ATF2 bound to TIP60 significantly decreased following IR (Fig. 1*c*), although TIP60 levels remained unchanged (Fig. 1*d*). These findings suggest that ATF2 is part of the TIP60 complex and that association of the two proteins is reduced following IR-induced DNA damage.

To map TIP60 domains required for association with ATF2, we generated three TIP60 fragments (Fig. 2*a*) predicted to retain their original conformation based on the crystal structure of the yeast TIP60 homologue ESA1 (30). Although ATF2 did not interact with the TIP60 N terminus (residues 1–258 amino acids), it efficiently bound to the C terminus (residues 258–531 amino acids), which includes the catalytic MYST domain and the zinc finger region. A significantly weaker association was seen with the fragment containing only the zinc finger region (Fig. 2, *b* and *c*), suggesting that association with ATF2 requires TIP60 residues 368–513. Consistent with these findings, an intact TIP60 acetyltransferase domain has also been shown to be required for interaction with the Ets family transcription factor ETV6 (31). Collectively, these data suggest that TIP60 associates with ATF2 via the MYST domain.

ATF2 Association with TIP60 Decreases TIP60 Steady State Levels Prior to DNA Damage—To assess the role of the ATF2-TIP60 association, we monitored changes in levels of endogenous TIP60 in cells depleted of ATF2 by transfection with corresponding siRNA. ATF2 depletion caused a marked increase in TIP60 protein levels in these cells. Following IR, TIP60 levels increased and the siRNA-mediated inhibition of ATF2 had less affect on TIP60 protein levels (Fig. 3*a*). Conversely, ectopic expression of ATF2 markedly decreased TIP60 protein levels, an effect blocked by treatment of cells with the 26 S proteasome inhibitor MG132 (Fig. 3*b*, compare *lanes 2–4*). Overexpression of the RING finger E3 ligase RNF5 as a control did not alter TIP60 levels (Fig. 3*c, lane 3*), indicating that the effect of ATF2 on TIP60 steady state levels is specific. These data suggest that ATF2 facilitates proteasome-dependent degradation of TIP60.

We next examined the effect of ATF2 on TIP60 steady state levels before and after IR by expressing either wild type or a phosphomutant form of ATF2 (490/8 mutant) that cannot be phosphorylated by ATM (8). Whereas wild type ATF2 efficiently decreased TIP60 protein levels before IR (Fig. 3*d*, *lane 2*), this effect was reduced following IR (*lane 3*), which dimin-

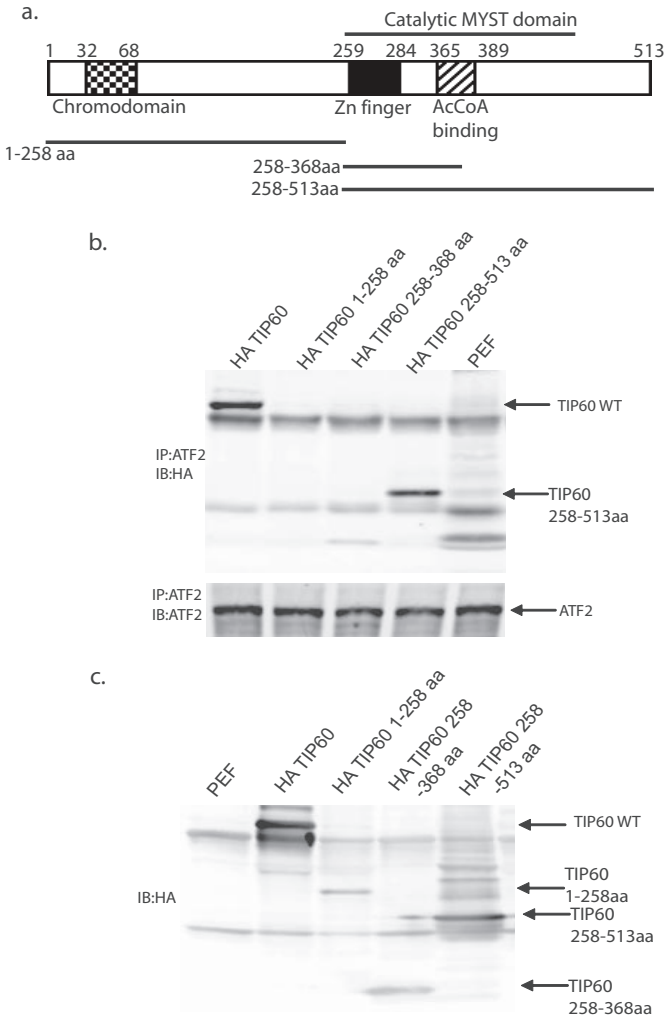

FIGURE 2. **Mapping ATF2 interaction with TIP60.** *a*, schematic illustration of TIP60 deletion constructs. *b* and *c*, mapping interaction of ATF2 with domains of TIP60. HA-tagged TIP60 deletion constructs were transfected into 293T cells. Varying amounts of the plasmids were transfected to enable equal expression of the different constructs. 24 h post-transfection cells were lysed and the nuclear fraction (500 μg) subjected to immunoprecipitation (*IP*) and immunoblotting (IB) with the indicated antibodies. *Panel c* shows levels of TIP60 deletion fragments, and *panel b* depicts association of ATF2 with these fragments.

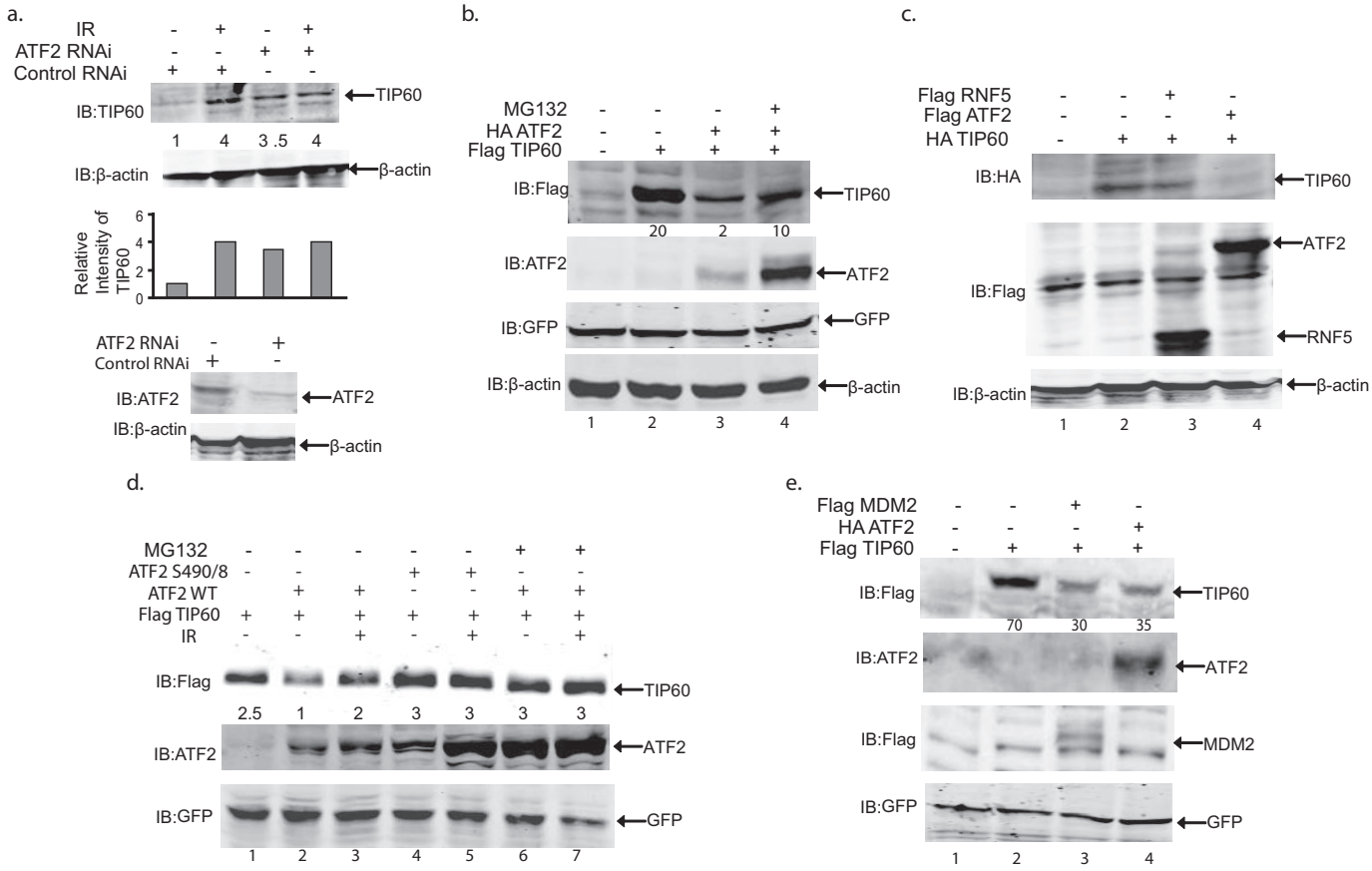

FIGURE 3. **ATF2 association with TIP60 limits steady state levels of TIP60 prior to DNA damage.** *a,* TIP60 protein levels increase upon inhibition of ATF2 expression. WM793 cells were transfected with 4 μg of vector control (pSuper) or ATF2 RNAi (pSuper ATF2). 48 h later cells were irradiated (5 Gray), and nuclear fractions prepared after 1 h. Steady state levels of endogenous TIP60 and β-actin are shown. Relative TIP60 protein levels were quantified using a Licor Odyssey scanner. The values of TIP60 levels normalized to β-actin are plotted in the histogram. Control for expression levels of endogenous ATF2 is shown in the *lower panel*. *b*, ATF2-mediated decreases in TIP60 steady state levels are attenuated by proteasome inhibition. FLAG-TIP60 and HA-ATF2 expression vectors (2 μg each) were transfected into 293T cells. 36 h later cells were treated with MG132 (40 μM; 5 h). Nuclear extracts (40 μg) were subjected to Western blotting using the indicated antibodies. Relative levels of TIP60 were quantified. *c*, ATF2 but not RNF5 mediates decreases in TIP60 steady state levels. HA-TIP60 and FLAG-ATF2 or RNF5 expression vectors (2 μg each) were transfected into 293T cells. Nuclear extracts (40 μg) were immunoblotted (*IB*) using the indicated antibodies. *d*, effect of ATF2 phosphomutants on TIP60 levels. Wild type FLAG-TIP60 and HA-ATF2 or HA-ATF2 S490/8 expression vectors (2 μg each) were transfected into 293T cells. 24 h later cells were treated with MG132 (40 μM). 5 h later cells were irradiated (5 Gray) and harvested after 1 h. The nuclear extract (40 μg) was subjected to Western blotting with the indicated antibodies. Relative levels of TIP60 protein were quantified. *e*, ATF2 decreases TIP60 steady state levels in p53/Mdm2 DKO cells. *P53/MDM2* double-null mouse embryonic fibroblasts were transfected with 2 μg of FLAG-TIP60, FLAG-MDM2, and HA-ATF2. After 36 h cells were harvested and the nuclear extract (60 μg) subjected to IB with anti-FLAG antibody (TIP60 and MDM2). The membrane was probed with ATF2 and GFP antibodies. Relative levels of TIP60 were quantified. *GFP*, green fluorescent protein.

ished the TIP60-ATF2 interaction (Fig. 1*b*). The reduction in TIP60 levels caused by ATF2 was blocked following treatment of cells with the 26 S proteasome inhibitor MG132 (*lane 6*). Conversely, expression of the ATF2 490/8 mutant did not mediate such a decrease prior to IR (Fig. 3*d*, compare *lanes 1*, *2*, and *4*), likely due to reduced association of the mutant form with TIP60 (supplemental Fig. S4, compare *lanes 1* and *3*). These data imply that even without IR ATF2 may be modified on ATM phosphoacceptor sites, albeit to a low level due to spontaneous damage and/or replication stress, and that such a modification may affect its ability to regulate TIP60 stability.

Earlier studies pointed to the role of MDM2 in the regulation of TIP60 stability (23). Indeed, TIP60 levels were reduced upon re-expression of MDM2 in mouse embryo fibroblasts derived from *Mdm2*$^{-/-}$/*P53*$^{-/-}$ double knock-out mice. Expression of ATF2 also reduced TIP60 protein levels in the absence of *Mdm2* (Fig. 3*e*). These data suggest that MDM2 is not required for the ATF2 effect on TIP60 stability.

Cul3 Is Required for ATF2-dependent Effect on TIP60 Stability—To search for candidate ligases that cooperate with ATF2 to reduce TIP60 stability, we employed the WebQTL data base, which consists of multiscale integration networks of genes, transcripts, and traits. This analysis ranked the E3 ubiquitin ligase Cullin3 (Cul3) (32) with high probability of being functionally linked with ATF2.

To test for an association between TIP60 and Cul3, cells were transfected with FLAG-TIP60 and Myc Cul3. Immunoprecipitation with FLAG antibodies followed by immunoblotting with Myc antibodies revealed association between exogenous TIP60 and Cul3 (Fig. 4*a*). Ectopic expression of FLAG-ATF2 and Myc-Cul3 identified an association between ATF2 and Cul3 (Fig. 4*b*). Because Cul3 is a scaffold protein of the E3 ligase complex that forms a catalytic core complex with ROC1/Rbx1/Hrt1 (32), we assessed the effect of Cul3 combined with ROC1 and/or ATF2 on TIP60 stability. Whereas Cul3 expression caused a moderate decrease in TIP60 levels, co-expression with ROC1 caused a

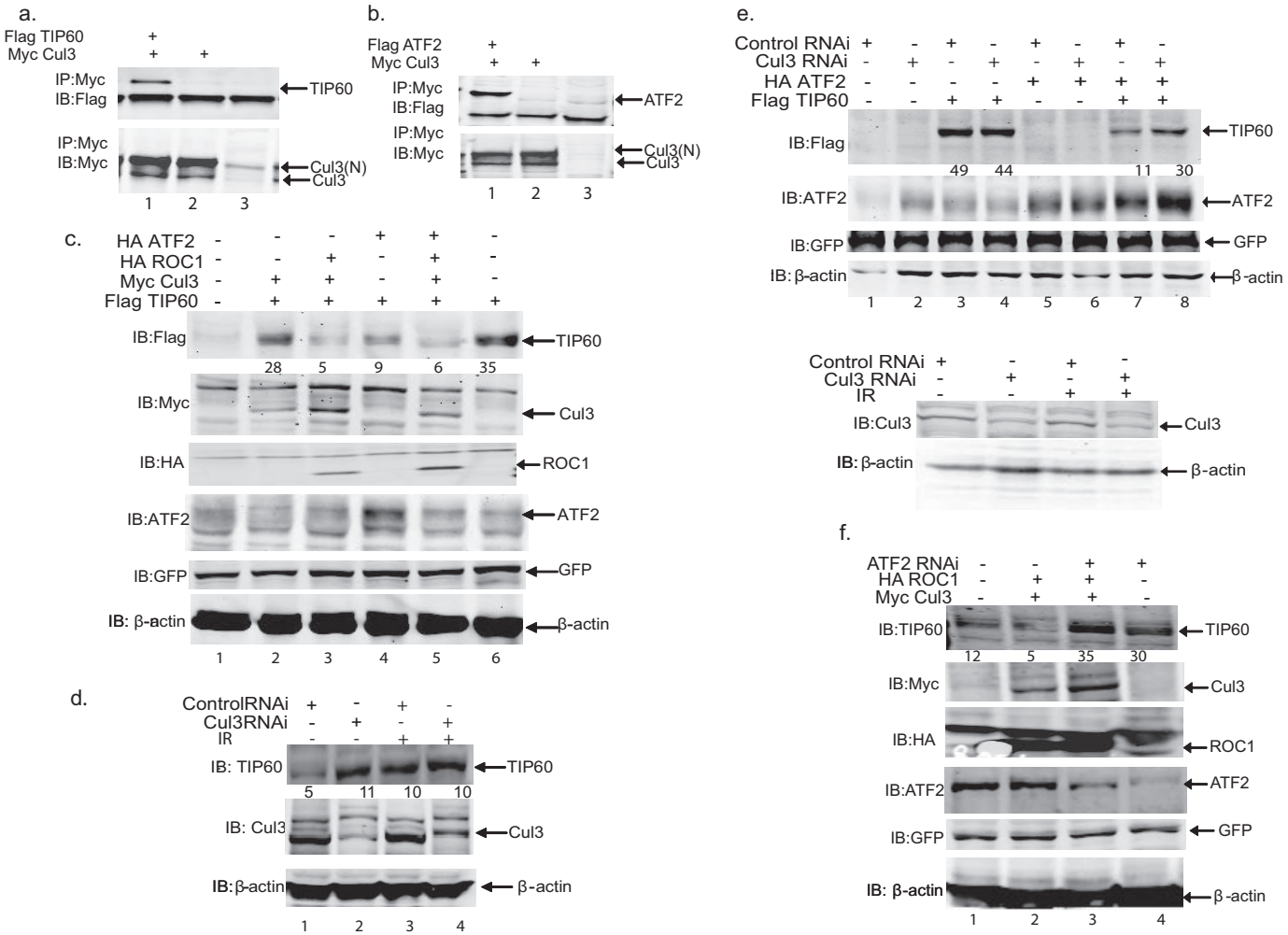

FIGURE 4. **Cul3 is required for ATF2-dependent effects on TIP60 stability.** *a* and *b*, Cul3 associates with ATF2 and TIP60. FLAG-ATF2, FLAG-TIP60, and Myc-Cul3 (3 μg each) were transfected into 293T cells. After 36 h cells were harvested and subjected to immunoprecipitation (*IP*) followed by immunoblotting (*IB*) with the indicated antibodies. Upper band denotes neddylated Cullin3(N). *c*, effect of Cul3, ROC1, and ATF2 on TIP60 steady state levels. 293T cells were transfected with 2 μg of FLAG-TIP60, Myc-Cul3, HA-ROC1, and HA-ATF2 in the indicated combinations. 36 h later cells were harvested and the nuclear extract (40 μg) subjected to IB with the indicated antibodies. The blot for ATF2 shows that the band for endogenous and exogenous ATF2 and that band intensity increases upon expression of exogenous ATF2. Relative levels of TIP60 were quantified. *d*, inhibition of Cul3 expression increases levels of endogenous chromatin-bound TIP60 before but not after IR. WM793 cells were transfected with a pool of siRNA oligos against *CUL3*. 60 h later cells were irradiated and harvested 1 h after IR. Nuclear extracts (75 μg) were subjected to IB with an anti-TIP60 antibody to detect endogenous TIP60 levels. Also shown are Cul3 and β-actin levels. Relative levels of TIP60 were quantified. *e*, inhibition of Cul3 expression attenuates ATF2-mediated degradation of chromatin-bound TIP60. HeLa cells were transfected with HA-tagged ATF2, FLAG-TIP60, and a pool of siRNA oligos against *CUL3*. Cells were harvested after 60 h, and the nuclear extract (70 μg) subjected to IB with anti-FLAG antibody. Also shown are levels of Cul3, green fluorescent protein (*GFP*), and β-actin. Relative TIP60 levels were quantified. *f*, inhibition of ATF2 expression attenuates Cul3-mediated degradation of TIP60. Cells were transfected with 2 μg of the vector control (pSuper) or ATF2 RNAi (pSuper ATF2 RNAi), Myc-Cul3, and HA-ROC1 as indicated. 48 h later cells were harvested and the nuclear fraction (75 μg) analyzed by IB using the indicated antibodies. Quantified levels of endogenous TIP60 are shown.

marked decrease in TIP60 steady state expression levels (Fig. 4*c*, compare *lanes 2* and *3*). ATF2 expression caused a marked decrease in TIP60 protein levels (Fig. 4*c*, *lane 4*). However, addition of ATF2 to the Cul3/ROC1 complex did not promote a further decrease in TIP60 levels over that seen with Cul3/ROC1 alone, possibly due to high expression of endogenous ATF2 in these cells. These data suggest that Cul3, in concert with ROC1, contributes to TIP60 degradation.

We next asked whether Cul3 is required for an ATF2-dependent decrease in TIP60 stability. Inhibiting Cul3 expression by Cul3 siRNA increased endogenous TIP60 levels (Fig. 4*d*, compare *lanes 1* and *2*). TIP60 levels increased after IR (Fig. 4*d*, *lane 3*) and inhibiting Cul3 expression no longer had any effect on endogenous TIP60 levels (Fig. 4*d*, compare *lanes 3* and *4*). These data suggest that Cul3 controls the levels of TIP60, but following IR, when interactions between ATF2 and TIP60 are reduced, Cul3 has little effect on TIP60 levels. Whereas Cul3 siRNA treatment was not sufficient to antagonize higher levels of overexpressed TIP60 (Fig. 4*e*), inhibiting Cul3 expression did attenuate the effect of ATF2 on TIP60 levels (Fig. 4*e*, compare *lanes 7* and *8*). These findings suggest that Cul3 is required for ATF2 to promote TIP60 degradation.

To directly address whether ATF2 is required for the effect of Cul3 on endogenous TIP60, we monitored changes in Cul3/ROC1-mediated TIP60 degradation in cells by decreasing endogenous ATF2 levels with siRNA. Although Cul3 and ROC1 expression markedly decreased TIP60 protein levels (Fig. 4*f*, compare *lanes 1* and *2*), this effect was blocked by ATF2

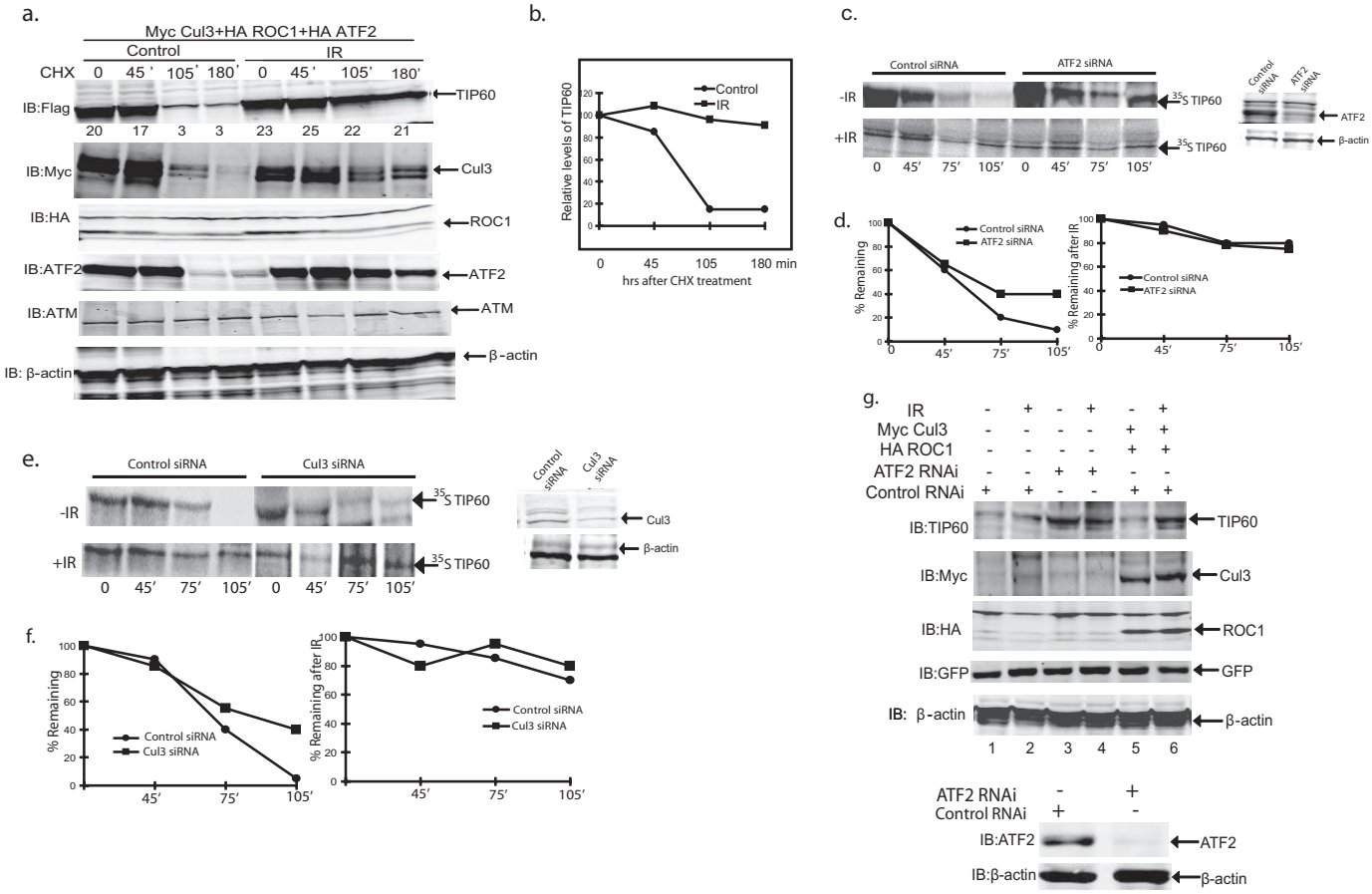

FIGURE 5. **Cul3-mediated degradation of TIP60 is attenuated after IR.** *a*, ATF2, Cul3, and ROC1 mediate efficient degradation of TIP60 before but not after IR. 293T cells were transfected with 2 μg of Myc-Cul3, HA-ROC1, and HA-ATF2. 36 h later cells were treated with cycloheximide (30 μg/ml; *CHX*). Cells were immediately irradiated (5 Gray) or mock-treated and harvested at the indicated time points. Immunoblotting (*IB*) was performed on whole cell extracts (40 μg) using anti-FLAG (TIP60) antibody. Also shown are levels of exogenous ATF2, ROC1, Cul3, and endogenous ATM and β-actin. Relative TIP60 protein levels were quantified. *b*, quantification of TIP60 degradation by ATF2/Cul3/ROC1 before IR. Data shown represent three experiments performed as described in *panel a*, which were quantified. *c* and *d*, WIDR cells were transfected with either control or ATF2 siRNA. TIP60 stability was evaluated in pulse-chase experiments by labeling for 45 min with [^{35}S]methionine/cysteine-containing medium (100 μCi/ml) and a subsequent chase with medium containing non-radioactive methionine and cysteine. Cells were lysed at 0, 45, 75, and 105 min after the chase and TIP60 immunoprecipitated with anti-TIP60 antibody. ^{35}S-Labeled TIP60 was analyzed with a Fuji FLA-5100 phosphorimager. The amount of [^{35}S]TIP60 is given as percent of control (100% at $t = 0$). The efficiency of ATF2 siRNA is shown on the *right panel*. *e* and *f*, same as *c*, except Cul3 siRNA was used. *g*, endogenous levels of TIP60 are affected by ATF2 and ROC1/Cul3 primarily prior to IR. M12 cells were transfected with 2 μg of the vector control (pSuper) or ATF2 RNAi (pSuper ATF2 RNAi), Myc-Cul3, and HA-ROC1 as indicated. 48 h later cells were irradiated (5 Gray) and harvested after 1 h; the nuclear fraction was isolated and used for IB (75 μg). Steady state levels of endogenous TIP60 and expression levels of endogenous ATF2, β-actin, Myc Cul3, HA ROC1, and green fluoriescent protein (*GFP*) are shown. Relative TIP60 protein levels were quantified. Efficiency of ATF2 siRNA is shown in *lower panel*.

depletion, which further increased TIP60 protein levels (Fig. 4*f*, compare *lanes 2* and *3*). This finding suggests that the Cul3/ROC1 effect on TIP60 stability is indeed ATF2-dependent.

Cul3-mediated Degradation of TIP60 Is Attenuated after IR—Because ATF2 and TIP60 association was reduced after IR, and given the role of ATF2 in the DNA damage response, we next compared the effect of ATF2 on TIP60 stability with and without IR. Given the role of Cul3 in mediating ATF2 effects and the fact that the maximal effects were seen upon expression of ROC1/Cul3/ATF2, this comparison was carried out following co-expression of these proteins. TIP60 half-life was markedly decreased by ATF2/Cul3/ROC1 expression in unirradiated cells ($t_{½}$ approximately 75 min) but not in irradiated cells (half-life >3 h; Fig. 5, *a* and *b*). Although ATF2 expression increased following IR (Fig. 5*a*) it no longer affected TIP60 stability, likely a result of post-translational modifications induced by IR (Fig. 3*d*).

To determine whether increases in endogenous TIP60 protein levels in the absence of ATF2 or Cul3 are attributable to increased TIP60 stability within the chromatin-bound fraction, we monitored TIP60 protein half-life in chromatin fractions. Immunoprecipitation of TIP60 from ^{35}S-labeled cells transfected with control siRNA, ATF2 siRNA, or Cul3 siRNA was performed at the indicated time points following pulse labeling. Chromatin-bound TIP60 exhibited a longer half-life in cells inhibited for ATF2 or Cul3 expression, compared with the control siRNA (Fig. 5, *c–f*). Moreover, TIP60 half-life increased following irradiation but was no longer affected following inhibition of ATF2 or Cul3 expression. Change in the migration of TIP60 seen at later time points may represent an ATF2-dependent modification (Fig. 5*f*). These results suggest that the half-life of chromatin-bound TIP60 is regulated by ATF2 and Cul3 prior to but not after irradiation.

Analysis of endogenous TIP60 levels confirmed an increase in their expression following IR or upon inhibition of ATF2

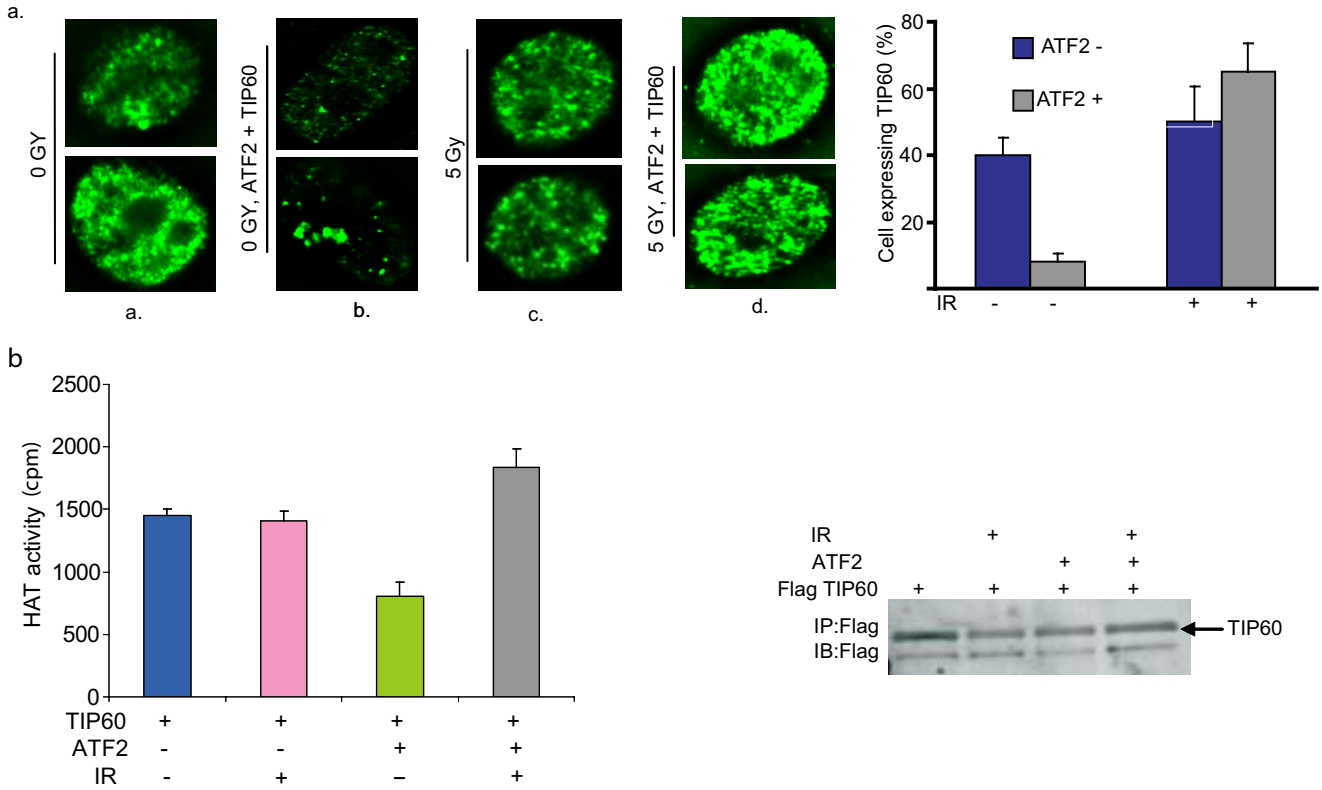

FIGURE 6. **ATF2 regulates protein levels and activity of TIP60.** *a*, immunostaining of TIP60 reveals reduced expression mediated by ATF2 prior to IR. HeLa cells were transiently transfected with 1 μg of FLAG-TIP60 and HA-ATF2 or control vector. 24 h later cells were mock treated or irradiated (5 Gray) and fixed after 1 h. Exogenous TIP60 localization was assessed by immunofluorescence using an anti-FLAG antibody. The *right panel* depicts quantification of cells expressing TIP60. *b*, ATF2 reduces the HAT activity of TIP60. 293T cells were transfected with FLAG-TIP60 and ATF2 (5 μg each) as indicated. 36 h later cells were irradiated (5 Gray) and harvested after 1 h and the chromatin-rich fraction was prepared. The TIP60 complex was immunoprecipitated (*IP*) from the chromatin-rich fraction in 0.15 M NaCl with affinity-purified anti-FLAG antibody cross-linked to protein A-Sepharose. TIP60 was eluted by addition of excess FLAG peptide and subjected to immunoblotting (*IB*) (*lower panel*) or assayed for HAT activity (*upper panel*). The HAT assay was performed as detailed under "Experimental Procedures" using a peptide derived from the N terminus of histone H4 and acetylation monitored using a modified enzyme-linked immunosorbent assay. Experiments were performed to assess changes in HAT activity levels by transfecting an empty vector and basal levels of HAT activity were measured before and after IR. Values from these analyses were considered background and were part of the quantification of TIP60 HAT activity presented here. The HAT assay was performed in triplicate and repeated twice. Shown are absolute levels of acetylation. Each *bar* represents the mean ± S.E. (n = 3) of all experiments.

expression by siRNA. Following IR, ATF2 association with TIP60 was reduced and its ability to affect TIP60 stability attenuated. The latter observation explains why overexpression of Cul3 and ROC1 (in presence of endogenous ATF2) no longer reduces TIP60 levels after IR (Fig. 5*g*, compare *lanes 5* and *6*).

The effect of ATF2 on TIP60 was also observed in cytological assays. Because we could not detect endogenous TIP60 using available antibodies, analysis was carried out using exogenously expressed proteins. TIP60 staining was seen in punctuate nuclear foci, which increased upon exposure to IR (Fig. 6*a*, compare *panels a* and *c*). TIP60 protein levels were reduced upon co-expression of ATF2 before IR but not in irradiated cells (Fig. 6*a*, compare *panels a* and *b*). Interestingly, TIP60 levels after IR were higher in the presence of ATF2 (Fig. 6*a*, compare *panels b* and *d*). TIP60 protein levels were detected in 10% of cells analyzed following ectopic expression of ATF2 *versus* 40% seen in control vector-expressing cells under non-stressed conditions. These data confirm that the effect of ATF2 on TIP60 stability is seen prior to IR and imply that ATF2 may elicit other changes on TIP60 following IR.

ATF2 Affects TIP60 HAT Activity—Because association between ATF2 and TIP60 required the catalytic MYST domain of TIP60, we next determined the effect of ATF2 on TIP60 HAT activity. Analysis was carried out on chromatin-bound fractions prepared from cells before and after IR exposure. Co-expression of ATF2 and TIP60 in 293T cells resulted in ~50% inhibition of HAT activity in immunopurified TIP60 prior to IR and increased HAT activity by ~20% after IR (Fig. 6*b*). These data suggest that elevated ATF2 levels affect TIP60 HAT activity before and after IR. Because the TIP60 levels were equal in each of these assays, the effect of ATF2 on TIP60 activity is likely to be independent of its contribution to TIP60 stability.

ATF2 Expression Levels in Human Tumors Affect TIP60 Protein Levels and ATM Activity—Earlier work from our laboratory indicated a role for ATF2 in melanoma development (33). We therefore assessed possible changes in TIP60 expression and ATM activity in human melanoma-derived cell lines. Consistent with earlier studies, ATF2 expression levels in this tumor type were high, although clear differences were also seen in expression levels of alternatively spliced forms of ATF2 (data not shown). Intriguingly, cells exhibiting high levels of full-length ATF2 also exhibited low levels of TIP60 expression and reduced ATM phosphorylation on serine 1981 following IR (Fig. 7, *a* and *b*, WM793 and FEMX cell lines). Cell lines derived from prostate cancer, lung cancer, and colon carcinoma cells also show inversely correlated TIP60 expression and ATM

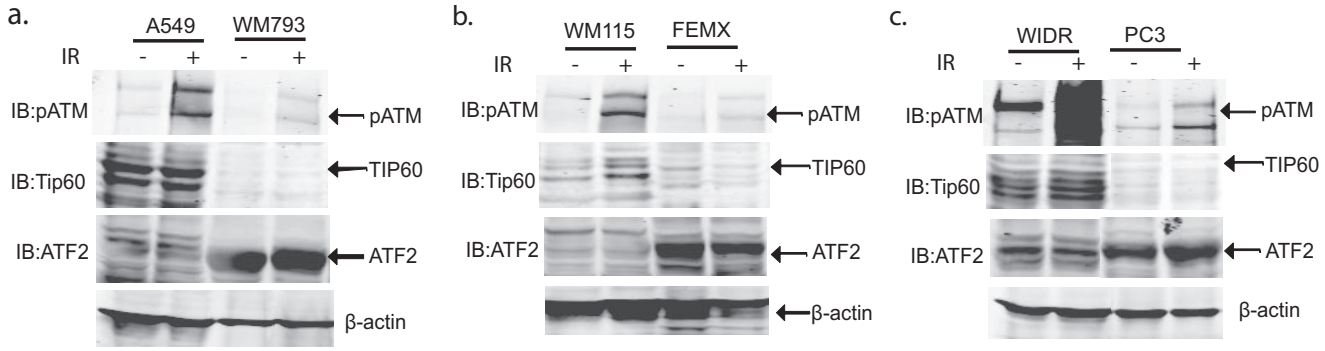

FIGURE 7. **Altered ATF2 expression in human tumors affects TIP60 protein levels and ATM activity.** *a–c*, analysis of ATF2, TIP60 protein levels, and ATM phosphorylation in human tumor-derived cell lines. A549 lung cancer or the indicated melanoma or prostate cancer lines were mock treated or irradiated (5 Gray) and harvested after 1 h. Cells were lysed and nuclear extracts (60 μg) were subjected to immunoblotting (*IB*) analysis to monitor endogenous pATM, TIP60, and ATF2 expression. The membrane was also probed with β-actin antibody to monitor equal loading.

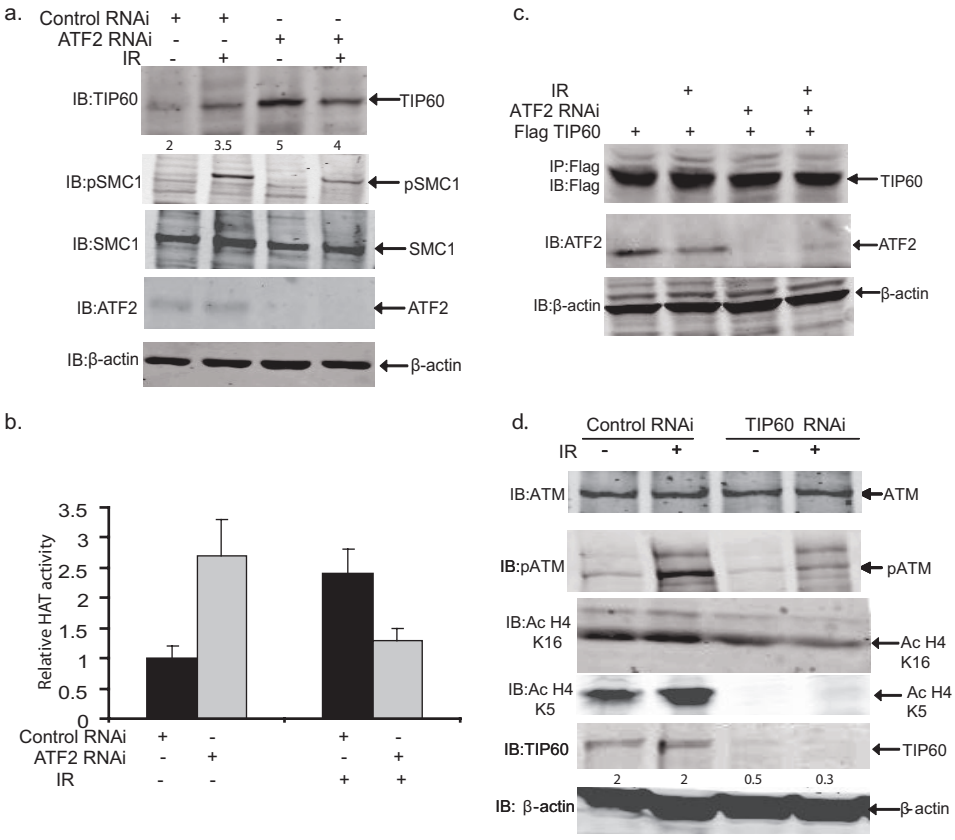

FIGURE 8. **Inhibition of ATF2 expression increases TIP60 HAT activity.** *a*, inhibition of ATF2 expression in human melanoma cells increases the TIP60 protein level and ATM activity. WM793 cells were transfected with 4 μg of the vector control (pSuper) or ATF2 RNAi (pSuper ATF2 RNAi). 48 h later cells were irradiated (5 Gray), and nuclear proteins prepared after 1 h were analyzed (75 μg) by immunoblotting (*IB*). Steady state levels of endogenous TIP60, pSMC1, and SMC1 are shown. The *lower panel* reveals the change in ATF2 levels upon RNAi. The membrane was also probed with β-actin antibody to monitor equal loading. *b* and *c*, ATF2 affect level of chromatin-bound TIP60 HAT activity. WM793 cells were transfected with 5 μg of FLAG-TIP60 in the presence or absence of ATF2 RNAi. 48 h later, cells were irradiated (5 Gray) and the chromatin-rich fraction prepared after 1 h was subjected to IB analysis (*panel c*) and HAT assay (*panel b*) using a modified ELISA as detailed under "Experimental Procedures." *d*, inhibition of TIP60 expression reduces ATM activation and H4 acetylation. HeLa cells were transfected with 4 μg of the vector control (pSuper) or Tip60 RNAi (pSuper TIP60 RNAi). 48 h later cells were irradiated (5 Gray), and the nuclear fraction prepared after 1 h was analyzed by IB. Steady state levels of endogenous ATM, pATM, Ac H4 K16, Ac H4 K5, and TIP60 are shown. The membrane was also probed with β-actin antibody to monitor equal loading. *IP*, immunoprecipitation.

activity, with high expression of full-length ATF2 (Fig. 7, *a* and *c*). RT-PCR analysis did not detect changes in TIP60 transcript levels, suggesting that variations in TIP60 expression among tumor-derived cell lines were at the protein level (Fig. S1). Because ATF2 localization was reported to be primarily nuclear in human melanomas (34), further analysis of a potential effect of ATF2 on TIP60 was carried out by monitoring ATF2 localization in these lines. Notably, in all cases ATF2 was primarily localized within cell nuclei (supplemental Fig. S2).

To directly assess the role of ATF2 in regulating TIP60 expression in tumor cell lines, we decreased ATF2 levels using corresponding siRNA and monitored levels of endogenous TIP60. Inhibiting ATF2 expression sufficed to increase TIP60 levels prior to IR and to a lesser degree after IR (Fig. 8*a*). The siRNA effect was also seen at the level of ATM activity, as measured by SMC1 phosphorylation, which, in agreement with our earlier observation, was moderately reduced after IR (8). RT-PCR did not detect changes in TIP60 transcript levels, suggesting that the effects of ATF2 are post-translational (supplemental Fig. S3).

Inhibiting ATF2 expression in WM793 cells caused a marked increase in TIP60 HAT activity prior to IR, suggesting that an excess of ATF2 limits expression and activity of TIP60 under normal growth conditions of these melanoma cells (Fig. 8*b*). It is important to note that equal amounts of TIP60 were used for the HAT assay, which rules out the possibility that reduced HAT activity was not due to decreased TIP60 levels (Fig. 8*c*). After IR, TIP60 levels were elevated, consistent with the increases seen in its HAT activity. However, inhibiting ATF2

under such conditions reduced TIP60 HAT activity (Fig. 8*b*), suggesting that ATF2 positively contributes to TIP60 activity after IR.

Elevated TIP60 expression and activity seen after IR could alter ATM activity (24). Consistent with this possibility we observed that inhibiting TIP60 expression by a corresponding siRNA resulted in a lower level of ATM phosphorylation and H4 K5, K16 acetylation (Fig. 8*d*). This finding suggests that ATF2 contributes to overall TIP60 protein levels and activity prior to and following IR, which affects the ability of TIP60 to activate ATM and acetylate histones.

DISCUSSION

The studies reported here reveal that TIP60 stability and activity are tightly regulated by the concerted action of ATF2 and Cul3/Roc1. We demonstrate that both ATF2 and Cul3/Roc1 are required for efficient degradation of TIP60, which limits availability and activity of this enzyme in the absence of DNA damage. Because TIP60 mediates important aspects of the DNA damage response through its effect on chromatin organization and ATM activity, our findings highlight a mechanism regulating ATM activation and histone modification.

The finding that ATF2-Cul3/Roc1 limits the stability and activity of chromatin-bound TIP60 extends our earlier finding that ATF2 is an ATM substrate playing an important role in intra-S phase checkpoint control following IR (8). Intriguingly, ATF2 was found also to affect levels of ATM activity, because inhibiting ATF2 expression decreased ATM phosphorylation on Ser-1981 (8), a marker of ATM activity. The present study reveals how ATF2 also contributes to the degree of ATM activation. Through control of TIP60, ATF2 limits ATM activation in cycling cells but increases ATM activity following IR. How does ATF2 contribute to TIP60 regulation? Clearly, ATF2 requires E3 ligase activity of Cul3/Roc1 to signal degradation of TIP60; similarly, Cul3/Roc1 requires ATF2 for its effect on TIP60. Yet, Cul3 also requires BTB domains containing proteins as part of the CUL3-ROC1 E3 ubiquitin ligase complex (35). Because ATF2 lacks a BTB motif, it is possible that a yet to be identified BTB-containing protein is part of this complex. Also plausible is that Cul3 assembles an atypical E3 complex, similar to what was shown for Dioxin receptor as part of the Cul4b ubiquitin ligase complex (36). ATF2 may serve as an adaptor to organize or recruit the Cul3/Roc1·TIP60 complex, or it may mediate contact with chromatin and/or DNA. ATF2 may also recruit additional regulatory proteins to this complex, possibly through its zinc finger or HAT-like domains. Mutation of either domain impedes the ability of ATF2 to affect the stability of TIP60.[3] ATF2 could also be subject to post-translational modification required for its effect on TIP60. Those may include acetylation, ubiquitination, or sumoylation, each of which is plausible given that ATF2 is acetylated, modified by ubiquitin, and known to associate with Ubc9, the SUMO-conjugating enzyme (37, 38). Independent of its effect on TIP60 stability, ATF2 also affects TIP60 HAT activity. The latter may be mediated by ATF2 association and interference with the

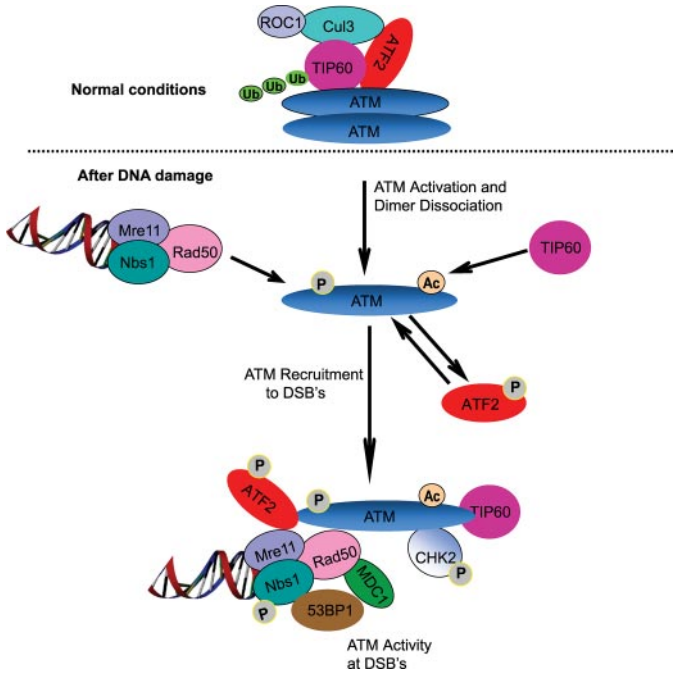

FIGURE 9. **Proposed model of ATF2 regulation of TIP60 and consequently ATM, before and after IR.** Under normal growth, ATF2 is assembled into a complex with TIP60 and Cul3, which also includes ATM. This results in degradation of TIP60, attenuating its ability to acetylate and activate ATM. Following DNA damage by IR, ATF2 dissociates from TIP60, enabling TIP60 acetylation and subsequent activation of ATM, with concomitant phosphorylation of ATF2 by ATM. Subsequently ATF2 is localized to DNA damage-induced foci and contributes to repair processes as well as the intra-S phase checkpoint.

TIP60 MYST domain, which mediates HAT activity. Intriguingly, while limiting HAT activity of TIP60 prior to DNA damage, ATF2 promotes TIP60 activity after IR, suggesting a change in the organization of the complex due to modification of either protein, or that the conformation/assembly of proteins within this complex enables an ATF2-mediated increase in TIP60 activity. Of note, ATF2 association with TIP60 is greater prior to DNA damage; after IR, ATF2 partially dissociates (up to 50%) from TIP60 in a dose-dependent manner.

Through regulation of the HAT activity of TIP60, ATF2 likely alters transcriptional programs. Given that ATF2 is activated by phosphorylation by the stress kinases JNK or p38, it is plausible that association with TIP60 would alter expression of a subset of genes transcriptionally regulated by ATF2 and its associated TIP60, as was shown for another component of the TIP60 complex, TIP49b (27).

The importance of ATF2 in TIP60 regulation is illustrated in human tumors where such regulation is impaired. We show here that regulation of TIP60 and consequently ATM activity are ATF2-dependent, because inhibiting ATF2 expression with corresponding siRNA sufficed to restore TIP60 levels and a degree of ATM activity. The present study provides an undisclosed link to explain impaired chromatin organization and DNA damage responses in human tumors where ATF2 overexpression inhibits TIP60 activity and protein levels. One would expect ATF2 function in the DNA damage response would be impaired in such tumors, because ATM activity, which is required for the contribution of ATF2 to this process, is reduced by decreased TIP60 availability and activity. Limiting

[3] A. Bhoumik, N. Singha, M. J. O'Connell, and Z. A. Ronai, unpublished observations.

the level of ATF2 expression should thus relieve the degree of inhibition and restore TIP60-dependent chromatin organization and ATM activity. Limiting ATF2 nuclear localization or its association with TIP60 may serve as a novel strategy to treat tumors in which ATF2 overexpression limits TIP60 availability.

Based on the present studies, we suggest that ATF2 is part of a feed-forward loop regulating availability and activity of TIP60, which in turn is required to activate ATM. Thereafter, ATF2 requires ATM for its localization within DSB repair foci and for its contribution to intra-S phase checkpoint control (Fig. 9). This model distinguishes between the activities of ATF2 in the absence of DNA damage and those following IR. Prior to IR ATF2 primarily serves to limit TIP60 activity, through which it controls TIP60-dependent acetylation. However, after formation of DSB by IR, ATF2 dissociates from TIP60, enabling an increase in TIP60 stability, and activity. Consequently, increased ATM activity serves to activate sensor and mediator proteins functioning in DNA damage responses. Among the substrates of ATM is ATF2, which when phosphorylated on residues 490 and 498 colocalizes with the MRE11 complex in DSB repair foci and contributes to the intra-S phase checkpoint. The role of ATF2 in regulating TIP60, in addition to its transcriptional activities and DNA damage response function, may vary with its localization within distinct functional complexes in different subcellular pools. For each function ATF2 likely requires different post-translational modifications, some of which are known (JNK or ATM phosphorylation on N- or C-terminal sites), whereas others await further studies.

Acknowledgments—We thank Reuven Agami for providing the pSuper and pRetro super constructs, Dan Mercola and Eileen Adamson for providing prostate cancer cell lines, Meenhard Herlyn for the melanoma cell lines, Ø. Fodstad for the FEMX and HHMSX cells, Yoshihiro Nakatani for TIP60 constructs, Zhen-Qiang Pan for Cul3 and ROC1 expression vectors, Yossi Shiloh for the ATM antibody, and Jiri Bartek, Jiri Lucas, John Petrini, and Bob Abraham for most helpful advice. We also thank members of the Ronai lab for discussions.

REFERENCES

1. Shiloh, Y. (2003) *Nat. Rev. Cancer* **3,** 155–168
2. Bakkenist, C. J., and Kastan, M. B. (2003) *Nature* **421,** 499–506
3. Kim, S. T., Lim, D. S., Canman, C. E., and Kastan, M. B. (1999) *J. Biol. Chem.* **274,** 37538–37543
4. Lim, D. S., Kim, S. T., Xu, B., Maser, R. S., Lin, J., Petrini, J. H., and Kastan, M. B. (2000) *Nature* **404,** 613–617
5. Matsuoka, S., Huang, M., and Elledge, S. J. (1998) *Science* **282,** 1893–1897
6. Sorensen, C. S., Syljuasen, R. G., Falck, J., Schroeder, T., Ronnstrand, L., Khanna, K. K., Zhou, B. B., Bartek, J., and Lukas, J. (2003) *Cancer Cell* **3,** 247–258
7. Anderson, L., Henderson, C., and Adachi, Y. (2001) *Mol. Cell. Biol.* **21,** 1719–1729
8. Bhoumik, A., Takahashi, S., Breitweiser, W., Shiloh, Y., Jones, N., and Ronai, Z. (2005) *Mol. Cell* **18,** 577–587
9. Li, S., Ting, N. S., Zheng, L., Chen, P. L., Ziv, Y., Shiloh, Y., Lee, E. Y., and Lee, W. H. (2000) *Nature* **406,** 210–215
10. Lou, Z., Minter-Dykhouse, K., Wu, X., and Chen, J. (2003) *Nature* **421,** 957–961
11. Bao, S., Tibbetts, R. S., Brumbaugh, K. M., Fang, Y., Richardson, D. A., Ali, A., Chen, S. M., Abraham, R. T., and Wang, X. F. (2001) *Nature* **411,** 969–974
12. Chen, M. J., Lin, Y. T., Lieberman, H. B., Chen, G., and Lee, E. Y. (2001) *J. Biol. Chem.* **276,** 16580–16586
13. Nakanishi, K., Taniguchi, T., Ranganathan, V., New, H. V., Moreau, L. A., Stotsky, M., Mathew, C. G., Kastan, M. B., Weaver, D. T., and D'Andrea, A. D. (2002) *Nat. Cell Biol.* **4,** 913–920
14. Siliciano, J. D., Canman, C. E., Taya, Y., Sakaguchi, K., Appella, E., and Kastan, M. B. (1997) *Genes Dev.* **11,** 3471–3481
15. Khanna, K. K., and Jackson, S. P. (2001) *Nat. Genet.* **27,** 247–254
16. Fisher-Adams, G., and Grunstein, M. (1995) *EMBO J.* **14,** 1468–1477
17. Ikura, T., Ogryzko, V. V., Grigoriev, M., Groisman, R., Wang, J., Horikoshi, M., Scully, R., Qin, J., and Nakatani, Y. (2000) *Cell* **102,** 463–473
18. Qin, S., and Parthun, M. R. (2002) *Mol. Cell. Biol.* **22,** 8353–8365
19. Tamburini, B. A., and Tyler, J. K. (2005) *Mol. Cell. Biol.* **25,** 4903–4913
20. Berns, K., Hijmans, E. M., Mullenders, J., Brummelkamp, T. R., Velds, A., Heimerikx, M., Kerkhoven, R. M., Madiredjo, M., Nijkamp, W., Weigelt, B., Agami, R., Ge, W., Cavet, G., Linsley, P. S., Beijersbergen, R. L., and Bernards, R. (2004) *Nature* **428,** 431–437
21. Kusch, T., Florens, L., Macdonald, W. H., Swanson, S. K., Glaser, R. L., Yates, J. R., 3rd, Abmayr, S. M., Washburn, M. P., and Workman, J. L. (2004) *Science* **306,** 2084–2087
22. Bird, A. W., Yu, D. Y., Pray-Grant, M. G., Qiu, Q., Harmon, K. E., Megee, P. C., Grant, P. A., Smith, M. M., and Christman, M. F. (2002) *Nature* **419,** 411–415
23. Legube, G., Linares, L. K., Lemercier, C., Scheffner, M., Khochbin, S., and Trouche, D. (2002) *EMBO J.* **21,** 1704–1712
24. Sun, Y., Jiang, X., Chen, S., Fernandes, N., and Price, B. D. (2005) *Proc. Natl. Acad. Sci. U. S. A.* **102,** 13182–13187
25. Murr, R., Loizou, J. I., Yang, Y. G., Cuenin, C., Li, H., Wang, Z. Q., and Herceg, Z. (2006) *Nat. Cell Biol.* **8,** 91–99
26. Neuwald, A. F., Aravind, L., Spouge, J. L., and Koonin, E. V. (1999) *Genome Res* **9,** 27–43
27. Cho, S. G., Bhoumik, A., Broday, L., Ivanov, V., Rosenstein, B., and Ronai, Z. (2001) *Mol. Cell. Biol.* **21,** 8398–8413
28. Brummelkamp, T. R., Bernards, R., and Agami, R. (2002) *Science* **296,** 550–553
29. Ogryzko, V. V., Kotani, T., Zhang, X., Schiltz, R. L., Howard, T., Yang, X. J., Howard, B. H., Qin, J., and Nakatani, Y. (1998) *Cell* **94,** 35–44
30. Yan, Y., Barlev, N. A., Haley, R. H., Berger, S. L., and Marmorstein, R. (2000) *Mol. Cell* **6,** 1195–1205
31. Putnik, J., Zhang, C. D., Archangelo, L. F., Tizazu, B., Bartels, S., Kickstein, M., Greif, P. A., and Bohlander, S. K. (2007) *Biochim. Biophys. Acta* **1772,** 1211–1224
32. van den Heuvel, S. (2004) *Curr. Biol.* **14,** R59–R61
33. Bhoumik, A., Huang, T. G., Ivanov, V., Gangi, L., Qiao, R. F., Woo, S. L., Chen, S. H., and Ronai, Z. (2002) *J. Clin. Investig.* **110,** 643–650
34. Berger, A. J., Kluger, H. M., Li, N., Kielhorn, E., Halaban, R., Ronai, Z., and Rimm, D. L. (2003) *Cancer Res.* **63,** 8103–8107
35. Furukawa, M., and Xiong, Y. (1995) *Mol. Cell. Biol.* **25,** 162–171
36. Ohtake, F., Baba, A., Takada, I., Okada, M., Iwasaki, K., Miki, H., Takahashi, S., Kouzmenko, A., Nohara, K., Chiba, T., Fujii-Kuriyama, Y., and Kato, S. (2007) *Nature* **446,** 562–566
37. Firestein, R., and Feuerstein, N. (1998) *J. Biol. Chem.* **273,** 5892–5902
38. Fuchs, S. Y., and Ronai, Z. (1999) *Mol. Cell. Biol.* **19,** 3289–3298